



كلية الهندسة - جامعة بغداد



اعضاء اتحاد الجامعات العربية

Performance Improvements of Filtered – OFDM based on Nuttall's filter

Zahraa Ali Jawad

Department of Electronics and Communication Engineering, University of Baghdad, Baghdad, Iraq, zahraa.ali@coeng.uobaghdad.edu.iq

* Corresponding author: Zahraa Ali Jawad

Published online: 30 September 2023

Abstract— Technology, particularly Internet of Things (IoT) and Machine Type Communication (MTC), have made a necessity to introduce a new distribution phenomenon. These innovations ask for very high data rates and non-coherent communication. When using inheritance 4th Generation (4G) frameworks, it is not possible to meet these requirements due to the inability to communicate without the use of synchronization. Numerous Orthogonal Frequency Division Multiplexing (OFDM) spectrum replacements, such as the Filtering-OFDM (F-OFDM), have been suggested. Due to the reduction in side-information required due to the synchronization application, a groundbreaking filter based on a minimum 4-term Blackman-Harris window defined by Nuttall is demonstrated numerically in this work. The recommended method outperforms previous design features in terms of spectral ability. In the F-OFDM transitional system, the root-raised-cosine filter is employed. This study, provided a new filter design that is simple to construct and can be completed in an immediate manner. Conventional Cyclic Prefix OFDM (CP-OFDM) showed -50.0 dBW/Hz, while the proposed scheme improved it to -253.2 dBW/Hz.

Keywords—5G, Nuttall-windowing, filtered-OFDM, OOB, Time/frequency localization, windowed-sinc filters.

1. Introduction

The recent 5G [7] project is expected to increase network congestion, such as tiny sensors found everywhere, which is one type of machine type communication (MTC), some types of sensors embedded in more sophisticated devices called internet of things (IoT) [12]. Banelli et al. revealed that variable harmonics are essential for future difficulties [20]. In 5G networks, signal synthesis reduces inconsistent delivery and protects big endpoints from expensive synchronization signaling [24, 23]. Subband orthogonality cannot be maintained in 4G networks using CP-OFDM modulation [26, 32]. 5G waveforms should be time-domain localized and independent of asynchronous transmission [28].

Filtered waveforms can be categorized into three categories: subcarriers, complete bands, and subbands. Waveforms based on subcarrier filtering [16], outperform CP-OFDM [18, 4, 31], which utilize staggered-quadrature amplitude modulation. The results are great, but the longer filter time-domain response decreases processing time (latency), which is important in 5G [30]. Intersymbol interference has decreased subcarriers-filtering orthogonality [6]. Spectral filtering using several subbands

per subband, its impulse response will be poorer than a per-subcarrier filter due to its output spectrum. This band was produced by LTE's 12 subcarrier resource blocks (RBs) [13, 15]. 5G's subband filtering-based universal filter multicarrier (UFMC) competed [23, 28, 30, 10]. Increase filter bandwidths to filter the entire conveyed subband range in one pass. The transmitter will only have one filter to deal with. Filtered-OFDM (F-OFDM) is the name given to this output waveform. F-OFDM will be the only focus of this research [29, 2]. Asynchronous communication simplifies OOB creation [14, 3, 1, 19, 11]. In [5, 9] they found that F-OFDM transmissions outperformed UFMC communications in packet delivery ratio and efficacy by using the same approach as [11].

To reduce OOB production even further, [3] suggests using a technique called "windowing-filtering" or "filtering-windowing," in which the filter and/or window investigated determines whether or not the goal is achieved. As a result, in the next part, we'll go over the design process and how new window designs were implemented. The layout that adopted in this article is as follows: the next section, 2, discusses filter design using windowing and a finite impulse response filter. The innovative signal structure of the F-OFDM mechanism, on

the other hand, will be based on a Nuttall-defined minimal 4-term Blackman-Harris-based filtering technique. Additionally, part 3 presents the results of the modeling exercise and discusses them, and section 4 contains the final comments.

2. Research Methodology and Proposal

The success of F-OFDM is strongly reliant on the filter design in order to achieve better temporal and frequency localization and hence boost network throughput. A basic and systematic methodology such as the windowed-sinc approach [17] may be applied online with little effort. The novel filter will be designed according to the following steps.

Step 1: In reality, this filter modeling approach contains a number of precisely articulated windows [22, 27], which are described below. This may be given numerically by:

$$z_n(n) = z_r(n) \cdot h(n) \quad (1)$$

The required time-domain response of the filter is denoted by $z_r(n)$. An optimal low-pass filter sinc output [8] might also be used to get the desired outcome. Thus, frequency domain application of the resulting filter necessitates that it must be shifted from its original location to somewhere in the center of the desired spectrum after windowing. The apparent Gibbs-issue [8] causes a ripple in the band's border spectrums as a result of this operation, takes time, which is due to the sinc-window filter's feature and the operation itself. As a result, ripple frequencies can be effectively eliminated by lengthening the designated spectrum for only a few subcarriers at the turnaround boundaries. As a result, frequencies flow straightest possible in chosen frequency bands meanwhile starting their roll-off at the envisioned limits.

As mentioned, the building procedure is vital, thus the filter technique's design must be careful when choosing a window function. Thus, OOB E can be reduced, improving time and frequency localization. In contrast to traditional CP-OFDM, the frequency range efficiency of CP-OFDM may be enhanced primarily by producing new bands that can be utilized to transmit useful information. As a result, data throughput rises as a result of this. According to the literature [22, 27], there are a variety of different types of windows, each having its own set of benefits and downsides. For instance, the rectangular-window mostly the fundamental of all window types. Since the rectangle function has poor frequency domain localisation, it has not been authorized for usage in 5G networks as a consequence of its principal drawback.

Step 2: By converging two rectangular windows, for example [27, 33], a triangular/Bartlett-window may be produced. With this in mind, it was decided to make windows with narrower main lobe widths and exceptionally shallow sidelobe depths as the final product. On the basis of the idea of [27], the authors fully

constructed other windows, to name some; convolution of the Hanning-window on its own [33] called Hanning-Hanning window. Consequently, it is mathematically possible to describe as

$$h_{new}(n) = h_1(n) \cdot h_2(n) \quad (2)$$

in this case, h_1 represents the first window and h_2 represents the second window.

Step 3: A novel window design is suggested in this study, with a smaller-width main lobe and fewer sidelobe grades than other windows previously published in the literature, as opposed to other windows now in use. With regard to state-of-the-art, it can be said that a minimal 4-term Blackman-Harris window developed by Nuttall has exceptionally low passband ripple. The window is regarded as lowest in the meaning that its greatest sidelobes are reduced [21]. The mathematical description of the Nuttall-defined minimal 4-term Blackman-Harris window is possible,

$$h_{Nut}(n) = \gamma_0 - \gamma_1 \cos\left[\frac{2\pi}{\varepsilon-1}n\right] + \gamma_2 \cos\left[\frac{4\pi}{\varepsilon-1}n\right] - \gamma_3 \cos\left[\frac{6\pi}{\varepsilon-1}n\right] \quad (3)$$

In which the coefficients γ_0 through γ_3 are replaced by the values 0.3635819, 0.4891775, 0.1365995, and 0.0106411, respectively [21], and the window size is denoted by the symbol ε .

Step 4: It follows from the abovementioned theory, and with the help of the expression of h_{new} in (2), developing a new window can be reached if frequency-domain convolution of Nuttall-window with the exact Nuttall-window, this corresponding to time-domain multiplication operation, according to Fourier Transform theory. To put it another way, according to (2), a new sample may be created simply multiplying $h_{Nut}(n)$ by itself without any more processing. Hence, the subsequent is how the new window, $h_{Nut2}(n)$, also known as Nut2-window, may be characterized, after some mathematical operations:

$$h_{Nut2}(n) = \mu_0 + \mu_1 \cos(\emptyset n) + \mu_2 \cos(2\emptyset n) + \mu_3 \cos(3\emptyset n) + \mu_4 \cos(4\emptyset n) + \mu_5 \cos(5\emptyset n) + \mu_6 \cos(6\emptyset n) \quad (4)$$

where

$$\emptyset = \frac{2\pi}{\varepsilon-1} \quad (5)$$

and $\mu_0, \mu_1, \mu_2, \mu_3, \mu_4, \mu_5,$ and μ_6 are listed in Table 1.

Table 1: Nut2-window coefficients.

Factor	Value
μ_0	0.26122544
μ_1	-0.42398714
μ_2	0.22418291

μ_3	-0.07455922
μ_4	0.0145351
μ_5	-0.00145357
μ_6	0.00005662

Step 5: It is necessary to employ this window in conjunction with the regular sinc-fuction in order to get the novel filter that is being discussed currently,

$$\rho(n) = \sin(\omega_c n)/(\omega_c n) \cdot w_{Nu}(n) \quad (6)$$

where ω_c is the frequency at which the signal is shut off.

Step 6: As a result, the F-OFDM signal may be expressed as,

$$y(n) = \left[\frac{1}{\sqrt{N}} \sum_{k=0}^{N-1} Y_i(k) e^{j2\pi \frac{kn}{N}} \right] * \rho(n) \quad (7)$$

The frequency indicator $k=0..N$ is used in the final statement. The F-OFDM transmission element viewing process starts with the acquisition of binary data and progresses from there. Data is altered based on the sequence in which the baseband modulation is applied by using M-QAM mapping. Inverse Fast Fourier Transform (IFFT) information is available after the serial to parallel transformation is done. Then the signal is converted from a parallel to a serial form via multiplexing. Figure 1 (upper-part) illustrates how the filter functionality will be performed as the last baseband process.

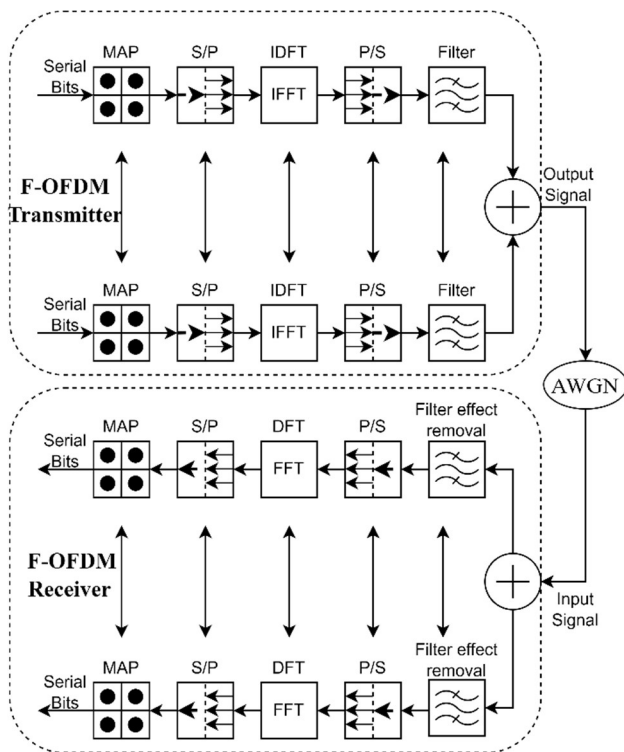


Figure 1: F-OFDM transmitter/receiver chain configuration setup [27]

Note that legacy OFDM is comparable to any individual chain seen in Figure 1, except it does not contain a filter. Figure 1 depicts the transmission process, while in the

traditional filtered OFDM/CP-OFDM, the receiving procedures are reversed as shown in Figure 1 (lower-part). The suggested filter devised in our work will therefore be shown to drastically reduce OOB leakage in a suggestive manner by the simulation results. In addition, the sidelobe will be far clearer, as will be seen in the next section.

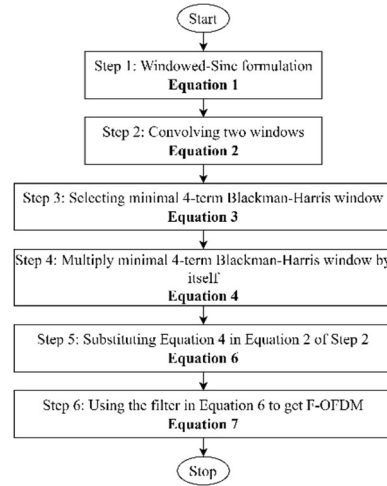


Figure 2: Suggested methodology procedure

That is, the approach employed in this work can be described in Figure 2, as just that the suggested filter (6) replaces the traditional filter of the F-OFDM structure to get the final mathematical model of the F-OFDM signal in (7).

3. Results and Discussions

To show the strong points of the suggested methodology, conventional OFDM and the traditional filtered OFDM will be simulated in a comparison manner in this section. In contrast, Nuttall's based filter will constitute the foundation of the proposed F-OFDM. According to Table 2 [27], the most important simulation parameters are presented here. There must be a significant number of Monte-Carlo repetitions to produce even somewhat correct results, as shown in Table 2.

Table 2: Parameters that are critical for F-OFDM simulation [27]

Parameter	Setting
N	1024
Monte-Carol rounds	10,000
Filter length (ϵ)	511
Number of subcarriers	12
Modulation order (M)	256-QAM
CP-Length	256
No. resource blocks	50
decay up/down (Tone offset)	2
Utilized channel	AWGN

With the intention of minimize disruption in synchronization-free telecommunications with changing numerology, the OOB leakage must therefore be lowered greatly, and this reduction must be large. Reasonably here to

incorporate the blocks represented in Figure 1 together into bigger system by utilizing the attributes provided in Table 2. It should be noted that the size of the Fourier Transform blocks is set at 1024 and that the filter length is 511 places [23, 32, 22]; in plenty of other terms, the IFFT size set at 1024 while the filter extends to $N/2-1$. Furthermore, the constellation map-order, denoted by the letter M , will be 256 levels, or 256-QAM. It is planned that there will be 50 RBs, each of which could feature exactly twelve subcarriers. In the decay-up/down transition stage, the tone-offset is two subcarriers long, corresponding to the decay-up/down phase. However, the receiving end of Figure 1 (upper-part) can be depicted in Figure 1 (lower-part). Thus, in Figure 1 (lower-part), the complete reverse of the operations in Figure 1 (upper-part) were achieved. Further, the CP-length is 25% of the total IFFT size, N , then, CP-length is 256. Using the Monte-Carlo approach, the experiment will be run for ten thousand trials. The proposed window time-domain structure can be recognized clearly in Figure 3.

With reference to Figure 3, Nut2 based new window shows improved behavior with in terms of mainlobe span as compared to that of Hanning or Hamming based structure. This enhancement is essential property that required in 5G transmitters and receivers. Figure 4 shows how the suggested window's frequency-domain compares to the frequency-domains of the Hamming and Hanning windows. In other words, as opposed to Hamming and Hanning windows, the spectrum intensity of the Nut2-window has the least sidelobe. Nut2-window's first sidelobe begins at -150dBW/Hz , while other windows are started at -61.56dBW/H and -56dBW/H correspondingly to Hamming and Hanning, respectively.

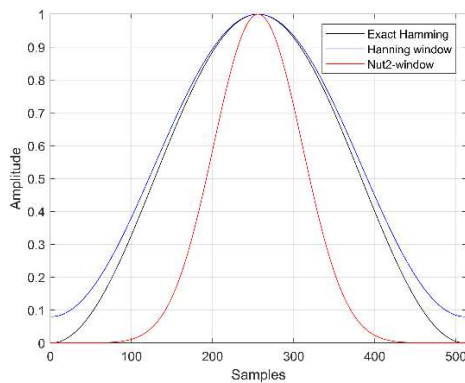


Figure 3: Time-domain representation of the proposed Nuttall-defined minimal 4-term Blackman-Harris window vs Hanning and Hamming windows

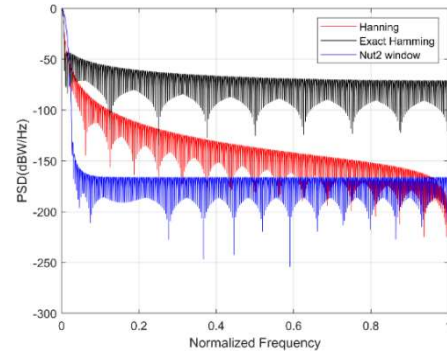


Figure 4: Nut2-window, Hanning-window, and Hamming-window frequency-domain plots comparison

F-OFDM-sidelobes in Figure 5, on the other hand, the Power Spectral Density (PSD) can be observed. Thus, based on Figure 5, the PSDs are -134.2 dBW/Hz and -50.0 dBW/Hz corresponding to Hamming-F-OFDM and legacy OFDM, respectively. This indicated the superiority of the Hamming-based F-OFDM methodology. Furthermore, the PSD result due to Hanning-Filtered OFDM format was lowered to -126.0dBW/Hz , this is an improved implementation of the F-OFDM signal, which is enhanced value as with respect to the conventional OFDM signal. Amazingly, the value was improved noticeably when employing Nut2 window to construct filtration to the OFDM signal, as depicted in Figure 5, is the lowest of the three (improved dramatically), it may be as low as -253.2dBW/Hz , which is an extremely improved signal relative to the legacy OFDM or any of the other windows used in this work.

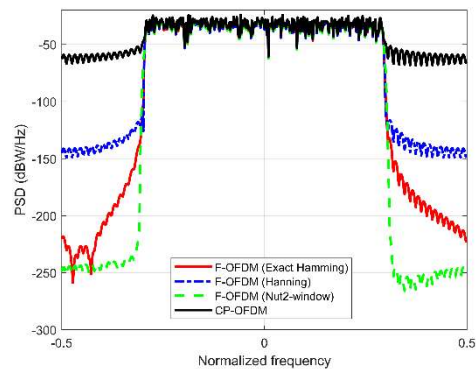


Figure 5: PSD of the OFDM compared to F-OFDM signals

As a result, the proposed window exhibits outstanding quality and may be adopted to suit the various kinds of transceivers needed by diverse communications technology, including MTC and URLLC systems, among others.

4. Conclusions

Better 5G networks with diverse numerology requirements need the use of synchronization-free connections. F-OFDM has the potential to be a competitor in this field. F-OFDM frequency/time localization has been pointedly amended when related to legacy OFDM pattern, thanks to the use of a novel filter design. This design, despite its increased complexity, has the advantage of being able to be implemented online while still maintaining the conventional filtering based OFDM architecture. Baseband modulation and symbol length are unrestricted in this production idea. Hence, it is recommended to use the suggested methodology in 5G communication technologies.

References

- [1] 3GPP LTE 36.104, G.T., "Base Station (BS) radio transmission and reception, in Evolved Universal Terrestrial Radio Access (E-UTRA)," 3GPP LTE 36.104, G.T. 2017.
- [2] Abdoli, J., M. Jia, and J. Ma., "Filtered OFDM: A new waveform for future wireless systems," 2015 IEEE 16th International Workshop on Signal Processing Advances in Wire-less Communications (SPAWC), 28 June-1 July 2015, Stockholm, Sweden.
- [3] An, C., B. Kim, and H. Ryu, "WF-OFDM (windowing and filtering OFDM) system for the 5G new radio waveform," 2017 IEEE XXIV International Conference on Electronics, Electrical Engineering and Computing (INTERCON), 15-18 Aug. 2017, Cusco, Peru.
- [4] Bedoui, A. and M. Et-tolba, "A comparative analysis of filter bank multicarrier (FBMC) as 5G multiplexing technique," 2017 International Conference on Wireless Net-works and Mobile Communications (WINCOM), 1-4 Nov. 2017, Rabat, Morocco.
- [5] Dan Wu, Xi Zhang, Jing Qiu, Liang Gu, Yuya Saito, Anass Benjebbour, Yoshihisa Kishiyama, "A Field Trial of f-OFDM toward 5G," 2016 IEEE Globecom Work-shops (GC Wkshps), 4-8 Dec. 2016, Washington, DC, USA.
- [6] Daoud, O., Hamarshah, Q., and Al-Sawalmeh, W., "MIMO-OFDM Systems Performance Enhancement Based Peaks Detection Algorithm," International Journal of Interactive Mobile Technologies (iJIM), vol. 7, no. 3, p. 4-8, Jun. 2013.
- [7] El Mahjoubi, A., Mazri, T., & Hmina, N., NB-IoT and eMTC: "NB-IoT and eMTC: Engineering Results Towards 5G/IoT Mobile Technologies," 2018 International Symposium on Advanced Electrical and Communication Technologies, November, Rabat, Morocco, 2018.
- [8] F. J. Harris, "Multirate signal processing for communication systems," second edition, CRC Press, New York, 2022.
- [9] Hu, K.C. and A.G. Armada., "SINR analysis of OFDM and f-OFDM for machine type communications," 2016 IEEE 27th Annual International Symposium on Personal, In-door, and Mobile Radio Communications (PIMRC), 4-8 Sept. 2016, Valencia, Spain.
- [10] Hussain, G.A. and L. Audah, "BCH codes in UFMC: A new contender candidate for 5G communication systems," Bulletin of Electrical Engineering and Informatics, vol. 10, no. 2, p. 904-910, Apr. 2021.
- [11] Jamal Bazzi, Petra Weitkemper, Katsutoshi Kusume, Anass Benjebbour, Yoshihisa Kishiyama, "Design and Performance Tradeoffs of Alternative Multi-Carrier Waveforms for 5G," 2015 IEEE Globecom Workshops (GC Wkshps), 6-10 Dec. 2015, San Diego, CA, USA.
- [12] Jeffrey G. Andrews, Stefano Buzzi, Wan Choi, Stephen V. Hanly, Angel Lozano, Anthony C. K. Soong, Jianzhong Charlie Zhang, "What Will 5G Be?" IEEE Journal on Selected Areas in Communications, vol. 32, no. 6, p. 1065-1082, Jun. 2014.
- [13] Jialing Li; Kenneth Kearney; Erdem Bala; Rui Yang, "A resource block based filtered OFDM scheme and performance comparison," ICT 2013, 6-8 May 2013, Casablanca, Morocco.
- [14] Jian Wang, Aixiang Jin, Dai Shi, Lei Wang, Hui Shen, Dan Wu, Liang Hu, Liang Gu, Lei Lu, Yan Chen, Jun Wang, Anass Benjebbour, Yoshihisa Kishiyama, "Spectral Efficiency Improvement With 5G Technologies: Results From Field Tests," IEEE Journal on Selected Areas in Communications, vol. 35, no. 8, p. 1867-1875, Jun. 2017.
- [15] Li, J., E. Bala, and R. Yang, "Resource block Filtered-OFDM for future spectrally agile and power efficient systems," Physical Communication, vol. 11, p. 36-55, Oct. 2014.
- [16] M. Bellanger, D. LeRuyet, D. Roviras, M. Terré, J. Nossek, L. Baltar, Q. Bai, D. Waldhauser, M. Renfors, T. Ihalainen, A. Viholainen, T. H. Stitz, J. Louveaux, A. Ikhlef, V. Ringset, H. Rustad, M. Najar, C. Bader, M. Payaro, D. Katselis, E. Kofidis, L. Merakos, A. Merentitis, N. Passas, A. Rontogiannis, S. Theodoridis, D. Triantafyllopoulou, D. Tsolkas, D. Xenakis, M. T. T. F. M. Huchard, J. Vandermot, A. Kuzminskiy, F. Schaich, P. Leclair, A. Zhao, "FBMC physical layer: a primer," PHYDYAS, p. 1-31, May 2010.
- [17] Mitra, S.K. and Y. Kuo, "Digital signal processing: a computer-based approach," McGraw-Hill New York, 2006.
- [18] Nicola Michailow, Maximilian Matthé, Ivan Simões Gaspar, Ainoa Navarro Caldevilla, Luciano Leonel Mendes, Andreas Festag, Gerhard Fettweis, "Generalized frequency division multiplexing for 5th generation cellular networks," IEEE Transactions on Communications, vol. 62, no. 9, p. 3045-3061. Aug. 2014.

- [19] P. Chaki, T. Ishihara, and S. Sugiura, "Precoded Non-Orthogonal Frequency Division Multiplexing with Subcarrier Index Modulation," in 2022 IEEE 95th Vehicular Technology Conference : (VTC2022-Spring), 2022, pp. 1-5.
- [20] Paolo Banelli; Stefano Buzzi; Giulio Colavolpe; Andrea Modenini; Fredrik Rusek; Alessandro Ugolini, "Modulation Formats and Waveforms for 5G Networks: Who Will Be the Heir of OFDM?: An overview of alternative modulation schemes for improved spectral efficiency," IEEE Signal Processing Magazine, vol. 31, no. 6, p. 80–93, Oct. 2014.
- [21] S. Choi, C.-W. Seo, and B. K. Cha, "Effect of Filtered Back-Projection Filters to Low-Contrast Object Imaging in Ultra-High-Resolution (UHR) Cone-Beam Computed Tomography (CBCT)," Sensors, vol. 20, p. 6416, 2020.
- [22] Sahrab, A.A. and A.D. Yaseen, "Filtered orthogonal frequency division multiplexing for improved 5G systems," Bulletin of Electrical Engineering and Informatics, vol. 10, no. 4, p. 2079–2087, Aug. 2021.
- [23] Schaich, F., T. Wild, and Y. Chen, "Waveform Contenders for 5G - Suitability for Short Packet and Low Latency Transmissions," 2014 IEEE 79th Vehicular Technology Conference (VTC Spring), 18-21 May 2014, Seoul, Korea (South).
- [24] Schwarz, S., T. Philosoph, and M. Rupp, "Signal Processing Challenges in Cellular-Assisted Vehicular Communications: Efforts and developments within 3GPP LTE and beyond," IEEE Signal Processing Magazine, vol. 34, no. 2, p. 47–59, Mar. 2017.
- [25] Shehab, J.N., H.R. Hatem, and O.A. Mahmood, "Hiding (1-8) Multimedia Files In One Color Image," Diyala Journal of Engineering Sciences, vol. 10, no. 3, p. 54–62, Sep. 2017.
- [26] Taher, M.A. and A.A. Mohammed, "Power Envelope Variation Improvement Of Downlink LTE System Using Complex Number Manipulation Approach," Diyala Journal of Engineering Sciences, vol. 8, no. 4, p. 618–623, Dec. 2015.
- [27] Taher, M.A., H.S. Radhi, and A.K. Jameil, "Enhanced F-OFDM candidate for 5G applications," Journal of Ambient Intelligence and Humanized Computing, vol. 12, p. 635–652. May 2021.
- [28] Wild, T., F. Schaich, and Y. Chen, "5G air interface design based on Universal Filtered (UF-)OFDM," 2014 19th International Conference on Digital Signal Processing, 20-23 Aug. 2014, Hong Kong, China.
- [29] Xi Zhang, Ming Jia, Lei Chen, Jianglei Ma, Jing Qiu, "Filtered-OFDM - Enabler for Flexible Waveform in the 5th Generation Cellular Networks," 2015 IEEE Global Communications Conference (GLOBECOM), 6-10 Dec. 2015, San Diego, CA, USA.
- [30] Xiaojie Wang, Thorsten Wild, Frank Schaich, Andre Fonseca dos Santos, "Universal Filtered Multi-Carrier with Leakage-Based Filter Optimization," European Wireless 2014; 20th European Wireless Conference, 14-16 May 2014, Barcelona, Spain.
- [31] Xudong Cheng, Yejun He, Baohong Ge, Chunlong He, "A Filtered OFDM Using FIR Filter Based on Window Function Method," 2016 IEEE 83rd Vehicular Technology Conference (VTC Spring), 15-18 May 2016, Nanjing, China.
- [32] Yinsheng Liu, Xia Chen, Zhangdui Zhong, Bo Ai, Deshan Miao, Zhuyan Zhao, Jingyuan Sun, Yong Teng, Hao Guan, "Waveform Design for 5G Networks: Analysis and Comparison," IEEE Access, vol. 5, p. 19282–19292, Feb. 2017.
- [33] Z. Q. Wang, G. Wichern, S. Watanabe, and J. L. Roux, "STFT-Domain Neural Speech Enhancement with Very Low Algorithmic Latency," IEEE/ACM Transactions on Audio, Speech, and Language Processing, vol. 31, p. 397-410, 2023.

Abbreviations

Adjacent-Channel-Interference	ACI
Bit Error Rate	BER
Conventional OFDM	CP-OFDM
Fifth Generation	5G
Filtering-OFDM	F-OFDM
Fourth Generation	4G
Generalized Frequency Division Multiplexing	GFDM
Internet of Things	IoT
Inverse Fast Fourier Transform	IFFT
Long Term Evolution	LTE
Machine Type Communication	MTC
Multi-Level-Quadrature Amplitude Modulation	M-QAM
Offset-Quadrature Amplitude Modulation	O-QAM
Orthogonal Frequency Division Multiplexing	OFDM
Out of band	OOB
Power Spectral Density	PSD
Resource Block	RB
Staggered-Quadrature Amplitude Modulation	S-QAM
Universal Filter Multi-Carrier	UFMC

تحسين اداء F-OFDM المستندة إلى مرشح الوقت الحقيقي

زهراء علي جواد

قسم الهندسة الالكترونية والاتصالات جامعة بغداد، zahraa.ali@coeng.uobaghdad.edu.iq

الباحث الممثل: زهراء علي جواد

نشر في: 30 ايلول 2023

الخلاصة – التطور المستمر في التكنولوجيا ، ولا سيما إنترنت الأشياء (IoT) ، والتقنيات الأخرى مثل اتصال نوع الآلة (MTC) ، جعلت من الضروري إدخال ظاهرة توزيع جديدة. تتطلب هذه الابتكارات معدلات بيانات عالية جداً واتصالات غير متماسكة أو نقل أقل تزامناً. عند استخدام أطر الجيل الرابع (G4) القديمة المدمجة ، والتي تم إنشاؤها حول الخاصية الرئيسية المتعامدة لتعدد الإرسال المتعامد بتقسيم التردد ، لا يمكن تلبية هذه المتطلبات نظراً لعدم القدرة على الاتصال دون استخدام التزامن ، أو متطلبات التحكم في النفقات العامة في شكل تكاليف تشغيلية للزمالة. العديد من بدائل الطيف OFDM (مضاعفة تقسيم التردد المتعامد) ، بما في ذلك استخدام مجموعة المرشحات من حيث الناقل متعدد الموجات ، أو FBMC (بنك المرشح متعدد الناقلات) ، أو GFDM (التعددية العامة لقسم التردد المتعامد) ، UFMC (تم اقتراح مرشح عالمي متعدد الحامل) وهو تعميم لجميع تقنيات الموجات الحاملة المتعددة القائمة على المرشحات مثل ترشيح (F-OFDM) ، وكلها تهدف إلى مطابقة متطلبات نظام الجيل التالي. نظراً لتقليص المعلومات الجانبية المطلوبة بسبب الحمل الزائد لتطبيق المزامنة ، يتم عرض عامل تصفية مبتكر يعتمد على حد أدنى من نافذة Blackman-Harris مكونة من 4 فصول تم تحديدها بواسطة Nuttall عددياً في هذا العمل. تتفوق الطريقة الموصى بها على ميزات التصميم السابقة من حيث القدرة الطيفية. في النظام الانتقالي F-OFDM ، يتم استخدام مرشح الجذر المرتفع لجيب التمام. من ناحية أخرى ، قدمت هذه الدراسة تصميم مرشح جديد سهل الإنشاء ويمكن إكماله بطريقة فورية. تم تصميم المرشحات المبتكرة على رأس المرشحات الترائية ، مما يعني أن الفلتر الجديد قد يستفيد من المزايا والعيوب المختلفة للفلتر السابقة مع إزالة عيوب المرشحات السابقة. أظهر CP-OFDM التقليدي -50.0 ديسيبل واط / هرتز ، بينما قام المخطط المقترح بتحسينه إلى -253.2 ديسيبل واط / هرتز.

الكلمات الرئيسية – الجيل الخامس ، Nuttall windowing ، F-OFDM ، انبعاث خارج النطاق ، توطين الوقت / التردد ، مرشحات نافذة-حقيقية الزمن.